Velocity profile of granular flows inside silos and hoppers

2005 J. Phys.: Condens. Matter 17 S2533

(http://iopscience.iop.org/0953-8984/17/24/011)

INSTITUTE OF PHYSICS PUBLISHING JOURNAL OF PHYSICS: CONDENSED MATTER

J. Phys.: Condens. Matter **17** (2005) S2533–S2548 doi:10.1088/0953-8984/17/24/011

Velocity profile of granular flows inside silos and hoppers

Jaehyuk Choi[1], **Arshad Kudrolli**[2] **and Martin Z Bazant**[1]

[1] Department of Mathematics, Massachusetts Institute of Technology, Cambridge, MA 01239, USA
[2] Department of Physics, Clark University, Worcester, MA 01610, USA

E-mail: jaehyuk@math.mit.edu, akudrolli@clarku.edu and bazant@math.mit.edu

Received 16 March 2005
Published 3 June 2005
Online at stacks.iop.org/JPhysCM/17/S2533

Abstract

We measure the flow of granular materials inside a quasi-two-dimensional silo as it drains and compare the data with some existing models. The particles inside the silo are imaged and tracked with unprecedented resolution in both space and time to obtain their velocity and diffusion properties. The data obtained by varying the orifice width and the hopper angle allow us to thoroughly test models of gravity driven flows inside these geometries. All of our measured velocity profiles are smooth and free of the shock-like discontinuities ('rupture zones') predicted by critical state soil mechanics. On the other hand, we find that the simple kinematic model accurately captures the mean velocity profile near the orifice, although it fails to describe the rapid transition to plug flow far away from the orifice. The measured diffusion length b, the only free parameter in the model, is not constant as usually assumed, but increases with both the height above the orifice and the angle of the hopper. We discuss improvements to the model to account for the differences. From our data, we also directly measure the diffusion of the particles and find it to be significantly less than predicted by the void model, which provides the classical microscopic derivation of the kinematic model in terms of diffusing voids in the packing. However, the experimental data are consistent with the recently proposed spot model, based on a simple mechanism for cooperative diffusion. Finally, we discuss the flow rate as a function of the orifice width and hopper angles. We find that the flow rate scales with the orifice size to the power of 1.5, consistent with dimensional analysis. Interestingly, the flow rate increases when the funnel angle is increased.

(Some figures in this article are in colour only in the electronic version)

1. Introduction

Granular materials display a surprisingly complex range of properties which make them appear solid- or liquid-like depending on the applied conditions [1, 2]. Because the interaction between the grains is dissipative and the thermal energy scale is small compared with the energy required to move grains, such materials quickly come to rest unless external energy is supplied constantly. Although vibro-fluidization and tumbling [3] is frequently used to excite granular materials, flows driven purely by gravity can occur in nature as well. Typical granular flows are dense and a fundamental statistical theory is not available to describe their properties. One reason for this situation is the lack of quantitative data which can be used to test and develop models of dense granular flow. In this paper, we focus on flows inside silos and hoppers in order to elucidate the nature of the flow and to test existing models. Such systems are ubiquitous due to the need to store and process granular materials in devices ranging from simple hour glasses to sophisticated nuclear pebble reactors [4, 5].

Several aspects of granular drainage have been studied over the years. Beverloo thoroughly investigated the relation between the orifice size and the mass flow rate in cylindrical silos and proposed a formula describing the observed dependence [6]. Using radiography, Baxter *et al* observed the density wave in the hopper flow and showed various patterns of the wave depending on the particle roughness and the hopper angle [7].

The velocity field of the flow inside a silo has been described by two different approaches. One is based on the critical-state theory of soil mechanics which relates stress and density to predict velocity field or mass flow rate [8, 9]. Although this approach has the appeal of starting from mechanical considerations, some questionable assumptions are made to resolve indeterminacy in the stress tensor, and the resulting equations are mathematically ill posed and can lead to violent singularities [10, 11]. The solutions available for hoppers possess shock-like velocity discontinuities ('rupture zones') [9], which are not seen in our experiments (see below).

The second approach ignores the stress field and attempts a purely kinematic description of the velocity profile, starting from an empirical constitutive law. A theory of this type was first discussed by Litwiniszyn, who introduced a stochastic model in which particles perform random walks through available 'cages' [12–14]. Later, Mullins independently proposed an equivalent stochastic model of the flow in terms of 'voids' and extensively developed the continuum limit, where a diffusion equation arises [15, 16]. Decades later, Caram and Hong revisited the void model and implemented it explicitly in computer simulations on a triangular lattice (where the voids are simply crystal vacancies) [17].

As an alternative to the microscopic void picture, Nedderman and Tüzün derived the same continuum equation starting from a constitutive law relating horizontal velocity and downward velocity gradient [18, 19]. Regardless of its derivation, the kinematic model predicts velocity fields with only one free parameter. In light of its simplicity, early experiments on silo drainage were viewed as successes of the model [19–21], even though it has since fallen from favour in engineering [9]. Although the free parameter has been observed to be proportional to grain diameter in all experiments, the constant of proportionality does not agree [19, 20, 22]. Furthermore, Medina *et al* [23] have reported that the kinematic parameter varies within a silo when the flow is analysed in detail by particle image velocimetry.

In addition to the studies of the flow pattern, the diffusion of particles has been investigated as well. Hsiau and Hunt [24] and Natarajan *et al* [25] imaged tracer particles in a dense flow inside a vertical channel with various boundary wall condition to investigate the concept of 'granular temperature'. From an analysis of velocity fluctuations, they found that particles shows normal diffusion and that the diffusivity in the stream-wise direction is higher than

in the transverse direction. Later, Menon and Durian used diffusing-wave spectroscopy to measure the dynamics of 100 μm glass beads inside a three-dimensional flow with improved temporal resolution, albeit at rather small length scales [26]. They reported that the particles show ballistic flight between collisions over a short timescale, and normal diffusion over a longer timescale, although the collision distance of 28 nm (1/10 000 of a grain diameter) could perhaps be associated with sliding or rotating asperities in frictional contacts. In any case, the randomizing gas-like collisions assumed in kinetic theories [27–29] have not been confirmed in any experiments on dense flows.

With rapid advances in high-speed digital imaging technology, it is now possible to simultaneously record thousands of individual particle positions with high spatial and temporal resolution. In a recent experiment by our group using this technique, the dynamics of 3 mm glass beads near a transparent wall in a three-dimensional silo was observed to be sub-ballistic but super-diffusive over short time intervals, and diffusive over long time intervals [30]. The data were argued to be consistent with slow cage rearrangement with particles remaining in long-lasting contacts by showing that the diffusion scaled only with distance travelled.

Therefore, inconsistencies can be noted in reported results which need to be resolved with thorough investigations. In the next section, we introduce the kinematic description of granular flow in silos and hoppers in detail. Since the stress field is not measured by imaging techniques, we do not assess critical-state mechanical models, aside from seeking the presence of the predicted shocks in the velocity field. Then, we outline the experimental set-up in section 3, and compare the prediction of models with our experiments in section 4. We discuss the implications of the comparison in section 5 and finally summarize the results in section 6.

2. Models for the mean velocity profiles

A simple kinematic description of the mean velocity profile in silos and hoppers has been developed since the 1950s, from a variety of theoretical perspectives [9]. The continuum kinematic model starts from an empirical constitutive law relating velocity components [18], which can be derived as a continuum limit of the (earlier) void model [12, 15]. The latter is a more complete theory, because it provides a microscopic mechanism for flow, which can be checked by experiments on diffusion and mixing. Recent experiments, however, have firmly rejected the void hypothesis. On the other hand, an alternative stochastic description, the spot model [31, 32], which starts from a cooperative mechanism for random-packing rearrangements, roughly preserves the mean flow profile of the kinematic model, with much less diffusion and slow cage breaking, consistent with experiments [30].

2.1. The kinematic model

Nedderman and Tüzün [18, 19] proposed a model based on the following constitutive law relating velocity components:

$$u = b\frac{\partial v}{\partial x}, \tag{1}$$

which states that the horizontal velocity u is proportional to the horizontal gradient (i.e. the shear rate) of the downward velocity v. This assumption is based on the fact that particles tend to drift horizontally towards a region of faster downward flow as they are likely to find more space to move in that direction. Assuming that the density fluctuation is small in dense granular regimes, they combined equation (1) with the incompressibility condition,

$$\frac{\partial u}{\partial x} - \frac{\partial v}{\partial z} = 0, \tag{2}$$

and obtained an equation for the downward velocity,

$$\frac{\partial v}{\partial z} = b\frac{\partial^2 v}{\partial x^2}. \tag{3}$$

Equation (3) has the form of a diffusion equation, where time is replaced by the vertical coordinate z. When an 'initial condition' is given for v at the bottom of the silo at $z = 0$, the velocity diffuses upward. The boundary condition assumed at the side walls of the silo is that the velocity is parallel to the wall. Although the authors did not discuss this situation, the condition can be naturally generalized to the case where the side walls are not vertical. It is written as

$$un_x - vn_z = 0 \qquad \text{at } (x, z) \text{ on the side wall,} \tag{4}$$

where (n_x, n_z) is the normal vector at the boundary.

For a semi-infinite quasi-two-dimensional system ($-\infty < x < \infty$) with a point-like orifice at $z = 0$ which acts as a source of velocity, a similarity solution exists:

$$v(x, z) = \frac{Q}{\sqrt{4\pi bz}}\mathrm{e}^{-x^2/4bz}, \tag{5}$$

where Q is the flow rate per unit thickness of the silo. We refer to the constant of proportionality b in equation (1), as the 'diffusion length', as it is has units of length. We provide a microscopic understanding of b in section 2.2.

The kinematic model has been tested experimentally, and the parameter b has been measured by various groups. Nedderman and Tüzün observed $b \approx 2.24d$ for various particle sizes [19]. Experiments by Mullins with monodisperse iron ore particles imply $b \approx 2d$ [20]. Medina *et al* used the particle image velocimetry (PIV) technique to obtain the velocity field and found that the diffusion length increases from $b \approx 1.5d$ to $\approx 4d$ as the height increases to fit the field [23]. Samadani *et al* reported $b \approx 3.5d$ for monodisperse glass beads using difference imaging to find velocity contours [22]. All the groups claimed that the prediction of the kinematic model qualitatively agreed with their experiment. The fact that a single fitting parameter b suffices to reproduce the entire flow field should be viewed as a major success of the kinematic model.

In order to test the kinematic model more thoroughly, we use numerical methods to solve the kinematic model subject to the same dimensions used in our experiments. For this purpose, we define the stream function, $\psi(x, z) = \int_0^x v(s, z)\,\mathrm{d}s$ and solve for $\psi(x, v)$ rather than $v(x, z)$. Formulated in terms of ψ, the boundary condition turns into a Dirichlet one from a rather complicated one given by equation (4). Furthermore, it is more convenient for the hopper geometry with inclined boundaries. If the width of the system is given by $L(z)$ and the silo is symmetric about its centre (e.g. $-L(z)/2 \leqslant x \leqslant L(z)/2$), the equation and the boundary condition for ψ are given by

$$\frac{\partial \psi}{\partial z} = b\frac{\partial^2 \psi}{\partial x^2} \qquad \text{and} \qquad \psi(0, z) = 0, \qquad \psi\left(\pm\frac{L(z)}{2}, z\right) = \pm\frac{Q}{2}. \tag{6}$$

We numerically integrate equation (6) from $z = 0$ using the Crank–Nicholson method to obtain the prediction of the kinematic model.

Due to its continuum formulation, the kinematic model cannot predict grain-level diffusion and mixing, so we now turn to statistical kinematic models for the velocity profile, which postulate mechanisms for random-packing dynamics.

2.2. The void model

Since equation (3) has the form of a diffusion equation, where the vertical distance z plays the role of 'time', it is clear that any microscopic justification for the kinematic model should be

based on independent random walks. In fact, this is how the model was first derived decades earlier, based on statistical considerations. Although the continuum approach is more general, in the sense that it is not tied to any specific microscopic mechanism, it lacks a clear physical basis, so it is important to consider what kind of microscopic mechanisms might support it.

Litwiniszyn first suggested the idea that particles are confined to a fixed array of hypothetical 'cages' as they perform random walks from one available cage to another during drainage [12–14]. Then, Mullins [15, 16] independently proposed an equivalent model in terms of 'voids' rather than particles, which is analogous to vacancy diffusion in crystals. In his model, particles move passively downward in response to the passage of voids, and the voids take directed random walks upward after emerging from the orifice.

Assuming that voids diffuse by non-interacting random walks, it is straightforward to show that in the continuum limit, at scales larger than the grain diameter, the concentration (or probability density) of voids, ρ_v, satisfies the diffusion equation,

$$\frac{\partial \rho_v}{\partial z} = b\frac{\partial^2 \rho_v}{\partial x^2}. \tag{7}$$

Since downward velocity v is proportional to the frequency of the void passage, this implies equation (3) of the kinematic model. However, the equivalence of the two model assumes that voids can be superimposed without interaction.

The void model also gives us an interpretation for the kinematic parameter, b. If a void undergoes a random horizontal displacement, Δx_v, while it climbs up by Δz_v, the parameter b is given by

$$b = \frac{\mathrm{Var}(\Delta x_v)}{2\Delta z_v}, \tag{8}$$

which is the characteristic length of the void diffusion. However, it is very difficult to determine b directly from equation (8). Δx_v and Δz_v cannot be measured from an experiment, nor does any *a priori* choice produce the measured value of b. Mullins also deduced $b \approx 2d$ from the velocity profile for round particles ($b \approx d/4$ for irregular particles) without specifying the value of Δx_v and Δz_v. By contrast, Caram and Hong [17] assumed a void makes an one-to-one exchange with particles on a regular lattice when they later revisited the void model. It is noteworthy that any regular lattice of hard-sphere packing under-predicts b ($b \ll d$) [31].

The void model faces more serious problems when it is used to predict diffusion and mixing, which was not done by its proponents. If a tracer particle is placed in a uniform flow driven by voids, the particle makes a directed random walk downward with precisely the same diffusion length as the voids moving up. Thus particles are easily mixed before they drop by a few particle diameters, which goes against our everyday experience and experiments (see below).

2.3. The spot model

To address these contradictions, Bazant *et al* [31, 32] proposed the spot model, which starts from a mechanism for cooperative diffusion in a dense random packing. It has roughly the same mean flow as in the kinematic model, because it also assumes that particles move in response to upward diffusing free volume, but this excess volume is carried in extended 'spots' of slightly enhanced interstitial volume, not in voids.

The kinematic parameter, b, is now set by the diffusion length for spots,

$$b = \frac{\mathrm{Var}(\Delta x_s)}{2\Delta z_s}, \tag{9}$$

where Δx_s and Δz_s are spot displacements in x and z directions, respectively. Unlike a void, which is a vacancy capable of being filled by an entire particle, however, a spot carries small fraction of interstitial space spread across an extended region and causes all affected particles to move (on average) as a block with the same displacement in the opposite direction to the spot.

Of course, there are more complicated internal rearrangements, which can be taken into account to achieve accurate spot-based simulations [33], but the simplest mathematical model already captures many essential features of dense drainage [31, 32]. For example, it is easy to see that the spot mechanism greatly reduces the diffusion length of particles, compared to the diffusion length of free volume. Suppose that a spot carries a total free volume V_s, and causes equal displacements $(\Delta x_p, \Delta z_p)$, among N_p particles of volume V_p. The particle displacement can be related to the spot displacement $(\Delta x_p, \Delta z_p)$ by an approximate expression of total volume conservation,

$$N_s V_p(\Delta x_p, \Delta z_p) = -V_s(\Delta x_s, \Delta z_s), \tag{10}$$

which ignores boundary effects at the edge of the spot. From this relation, we can compute the particle diffusion length,

$$b_p = \frac{\mathrm{Var}(\Delta x_p)}{2\Delta z_p} = \frac{w^2\,\mathrm{Var}(\Delta x_s)}{2w\Delta z_s} = w b_s \tag{11}$$

which is smaller than the spot diffusion length by a factor $w = V_s/N_p V_p$. This can in turn be related to the change, $\Delta\phi$, in local volume fraction, ϕ, caused by the presence of the spot,

$$w = \frac{b_p}{b} = \frac{V_s}{N_p V_p} \approx \frac{\Delta\phi^2}{\phi}. \tag{12}$$

It is well known from simulations and experiments that the volume fraction fluctuates on the order of 1% in a dense flow, so the spot model thus predicts $w = b_p/b = \mathrm{O}(10^{-2})$. (In our experiments, the local area fraction of glass beads near the viewing wall varies by less than three per cent.) The estimate of w is further reduced by noting that spots occur in large numbers and overlap, so that each spot contributes only a small part of the change in local volume fraction. We will test this prediction in our experiments.

3. Experimental procedure

3.1. Experimental set-up

Our experimental apparatus and procedure is similar to that used in our previous report [30]. We use black glass beads ($d = 3.0 \pm 0.1$ mm) in a quasi-two-dimensional silo with length $L = 20.0$ cm ($67d$), height $H = 90.0$ cm ($300d$), and thickness $D = 2.5$ cm ($8.3d$). The particles near the front wall of the silo are measured through the transparent glass. The slight polydispersity reduces the tendency for hexagonal packing to occur near the wall. The thickness of the silo D is large enough that finite-size effects are not significant. We obtain similar results for both mean velocity and diffusion when we increase D [30]. A distributed filling procedure was used to fill the silo with the grains. The orifice is opened and steady state flow is allowed to develop before acquiring the images used for determining particle positions.

We view a rectangular region of 20.0 cm × 50.0 cm above the orifice with a resolution of 256 × 1280 pixels. Therefore, each particle diameter corresponds to $d = 7.7$ pixels. The images are acquired at a rate of 125 frames per second. The camera memory allows 2048 consecutive images to be stored at this resolution and therefore the maximum interval over which we can track a particle is about 16.4 s.

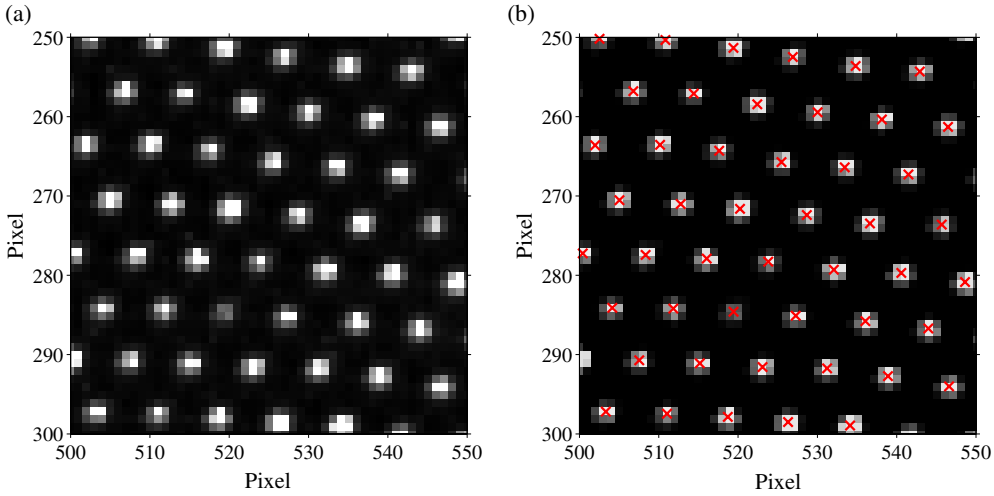

Figure 1. (a) A raw image of the glass beads acquired with the high-speed camera, and (b) the preprocessed image along with the position of the centroid of the identified particle (×).

For the funnels in the hopper, Plexiglass wedges are placed on top of the bottom plate. The surface property of wedge boundaries is identical to the side walls. We use wedges with three different angles, $\theta = 30°, 45°$ and $60°$. The orifice size $W = 18$ mm is fixed for the hopper experiments while it is varied to $W = 12$, 16 and 20 mm for the silo. To gain good statistics, three experiments are conducted for each funnel angle and orifice size. We also use data from a wider range of orifice sizes than acquired during our previous study [30] in section 4.2.

3.2. Particle tracking

To identify the locations of particles from images, we employ the algorithm proposed by Crocker and Weeks [34]. In this algorithm, the raw images are preprocessed to reduce the noise and the background. This involves convolving the image with a Gaussian filter and then an average filter of roughly d pixels respectively. The particle location is then identified with the centroid around the local maximum brightness pixel in the modified image. To optimize the particle tracking for our experiment, the algorithm was also further customized. Because the glass beads are circular, we use a circular shaped filter. We also set an intensity cut-off to discard the blur images of particles located far away from the front wall. A sample of an image before and after the processing is shown in figure 1. The position of the located particles is also superposed.

After particles are located frame by frame, their trajectories should be retrieved by 'connecting' their positions in time. We associate a particle in a frame with another in the next frame which is within a radius of $0.66d$ pixels around the original position. This simple method works well, avoiding more complicated multiple associations except very near the orifice where the particles move more than $0.66d$ pixels per frame. The particles can be tracked there by using a faster frame rate, but we do not do so here since bulk flow, and not orifice dynamics, is the focus of our study.

4. Analysis of the experimental results

4.1. Comparison of the measured velocity profiles with the kinematic model

We first compare the data from the flat-bottom silo with the model. Figure 2(a) shows the contour plot of the average downward velocity v. The mean velocity is obtained by dividing

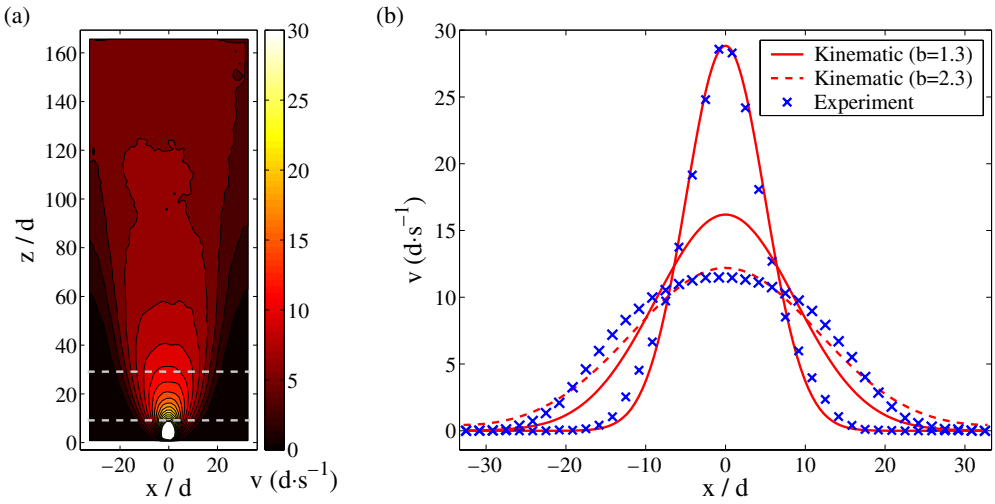

Figure 2. (a) Contour plot of the average downward velocity field, v, in a flat-bottomed silo with an orifice width, $W = 16$ mm. (b) v as a function of x at the two heights, $z_1 = 9.1d$ and $z_2 = 29.1d$ indicated with grey dotted lines in (a). The result from the kinematic model in the same geometry fits best with $b = 1.3d$ for the z_1 profile, and $b = 2.3d$ for the z_2 profile. The result from the model for the z_2 profile with b fitted at z_1 (narrow solid curve) is also shown.

the observation window into square cells of size $1.6d \times 1.6d$. Then in each cell the average is performed over the displacements of all the particles passing through the cell. We again take the average of the field from three experiments. The data across experiments show little variation, which confirms that the velocity field is well defined and stationary. Thus we do not show the error bar in the plots of this paper unless the concerned quantity has visible fluctuations.

The contour plot shows that v is a maximum right at the orifice and appears to 'diffuse' upward, in qualitative agreement with the models discussed above. The regions in the left and right corners made by the side walls and the bottom plate remain stagnant, and the boundary of the mobile region has a parabolic shape. In figure 2(b), we show the profiles $v(x)$ at two cross sections $z_1 = 9.1d$ and $z_2 = 29.1d$ (dotted lines in figure 2(a)) with the fit to the kinematic model. The diffusion length, $b = 1.3d$, was the best fit for the profile at z_1. However, b becomes larger when z increases as some previous reports have also shown [9, 23]. The profile at z_2 is best fitted with $b = 2.3d$, but it has a flattened shape at the centre with a thinner tail indicating further obvious deviations from the model.

The velocity profiles from the experiments with different orifice widths turn out to coincide when they are normalized by the flow rate as is commonly observed in other dense granular flows [35]. Thus the best fitting value of b is independent of the flow rate. The dependence of the flow rate on the orifice width will be discussed in the next subsection.

We performed similar analysis of the experiments with the hoppers. The contour plots along with the profiles at $z = z_1, z_2$ for the angles 30°, 45° and 60° are presented in figures 3–5 respectively. As the angle is increased, the stagnant region is diminished as the particles slip on the wedge. At z_1 the critical angle over which slip occurs is between 30° and 45°, and at z_2 it is between 45° and 60°. However the shape of equi-velocity contours well above the funnel is not affected significantly by the funnel's detailed shape.

The value of b to obtain the best fit depends on the angle of the hopper as well. It increases from $2.1d$ to $2.8d$ for z_1, and from $2.6d$ to $4.5d$ for z_2 as the angle is increased.

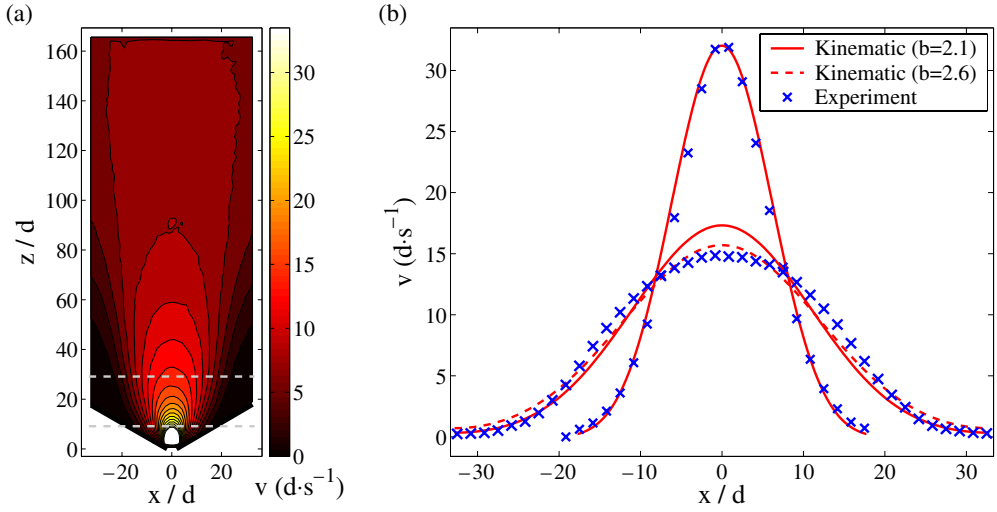

Figure 3. (a) Contour plot of the average downward velocity field, v, in a hopper with angle, $\theta = 30°$, and $W = 18$ mm. (b) v as a function of x at the two heights, $z_1 = 9.1d$ and $z_2 = 29.1d$, indicated with grey dotted lines in (a). The result from the kinematic model fits best with $b = 2.1d$ for the z_1 profile and $b = 2.6d$ for the z_2 profile. The result from the model for the z_2 profile with b fitted at z_1 (narrow solid curve) is also shown.

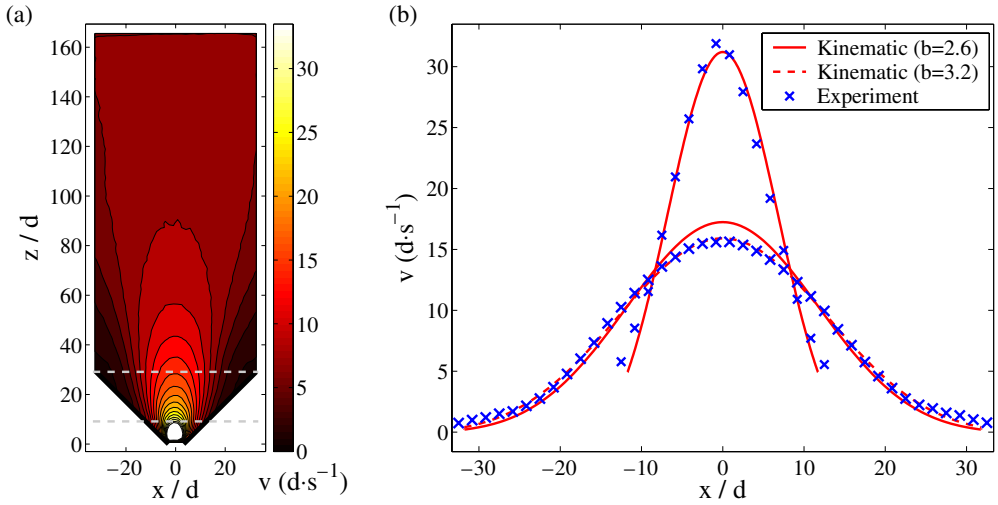

Figure 4. (a) Contour plot of the average downward velocity field, v, in a hopper with angle, $\theta = 45°$, and $W = 18$ mm. (b) v as a function of x at the two heights, $z_1 = 9.1d$ and $z_2 = 29.1d$, indicated with grey dotted lines in (a). The result from the kinematic model fits best with $b = 2.1d$ for the z_1 profile and $b = 2.6d$ for the z_2 profile. The result from the model for the z_2 profile with b fitted at z_1 (narrow solid curve) is also shown.

Although we observe some quantitative discrepancies with the simple kinematic model with a constant coefficient, b, the flow is at least qualitatively consistent. This appears not to be the case with continuum models from critical-state soil mechanics [9], which generally predict sharp, shock-like discontinuities in velocity (and stress, which we do not measure) within the

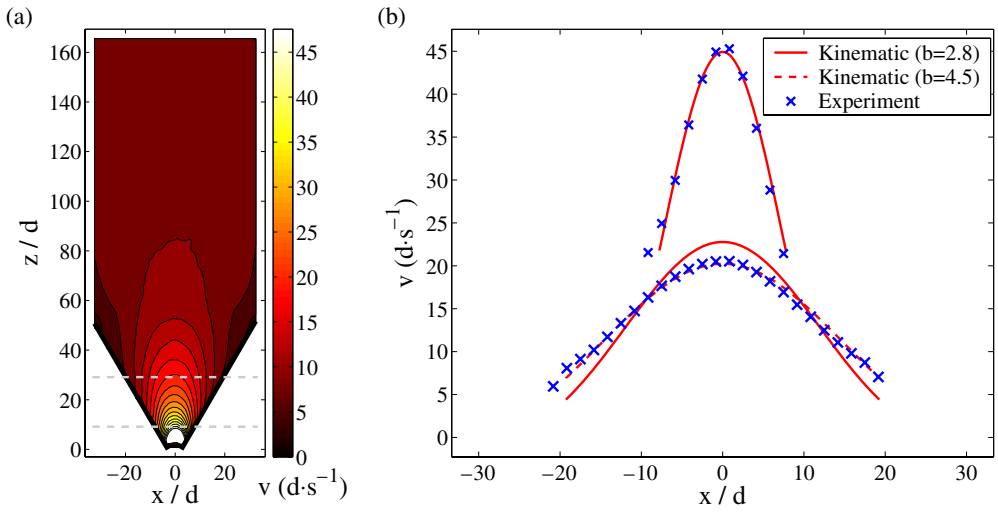

Figure 5. (a) Contour plot of the average downward velocity field, v, in a hopper with angle, $\theta = 60°$, and $W = 18$ mm. (b) v as a function of x at the two heights, $z_1 = 9.1d$ and $z_2 = 29.1d$, indicated as grey dotted lines in (a). The result from the kinematic model fits best with $b = 2.6d$ for the z_1 profile and $b = 3.2d$ for the z_2 profile. The result from the model for the z_2 profile with b fitted at z_1 (narrow solid curve) is also shown.

silo, especially near corners. We see no such abrupt jumps in velocity in the silo, only rather smooth velocity profiles.

4.2. Flow rate dependence on the orifice size and the funnel angle

The mass flow rate in a silo during discharge was an important subject of early research. Using drainage experiments in cylindrical silos with a circular orifice, Beverloo *et al* [6] reported a relation known as the Beverloo correlation

$$Q \propto \rho\sqrt{g}(W - kd)^{2.5}, \qquad k = 1.4 \tag{13}$$

where Q is the mass flow rate, ρ is the bulk density of packing, g is the gravitational constant and W is the diameter of the orifice. It is usually argued that $Q \propto \rho\sqrt{g}(W - d)^{2.5}$ is the only form which can be deduced from the dimensional analysis as $(W - d)$ is the effective diameter (or width) where particle centres can be placed within the orifice, but arching and other effects could also introduce the particle diameter d and thus another dimensionless parameter, d/W. Instead, the Beverloo correlation includes a somewhat controversial factor $W - kd$, where the empirical factor k is claimed to derive from the region near the orifice rim which obstructs the passage of particles. This picture could be consistent with the concept of an 'empty annulus' proposed by Brown and Richards [36].

For a *slit* orifice with a quasi-two-dimensional silo as in our experiment, the dependence can be obtained to be

$$Q \propto \rho\sqrt{g}(D - d)(W - kd)^{1.5}, \tag{14}$$

because the flow rate is linear with system depth $D - d$.[3] We investigated the flow rate dependence on orifice width using our data. Although the discharged mass flux is not directly measured, we use the overall average velocity, $v^* = Q/L$, to obtain the flow rate.

[3] It should be noted that the orifice in our system is entirely open from front to back surface. Thus the 'empty annulus' argument is difficult to apply in the direction of silo depth. We cannot find the exact dependence on D because we fix $D = 2.5$ cm.

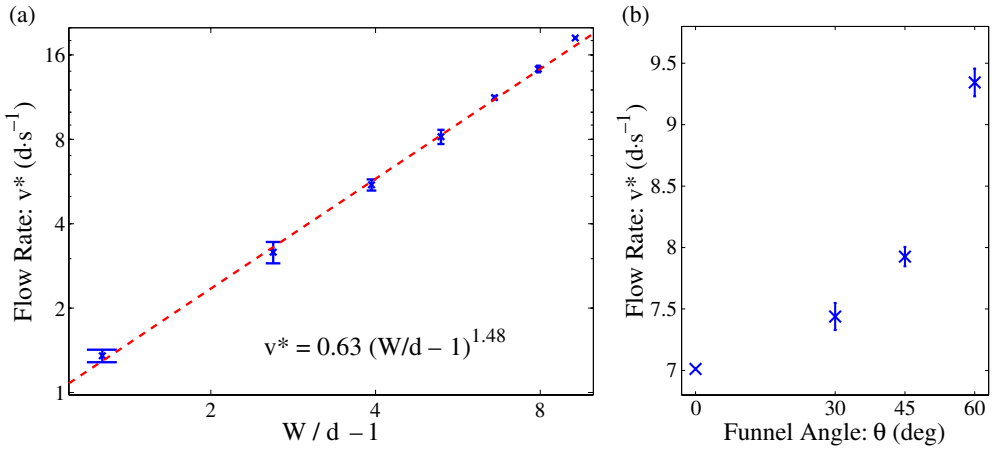

Figure 6. The dependence of flow rate on (a) the effective orifice width, $W/d-1$, in a flat-bottomed silo (log–log scale), and (b) the funnel angle θ in a hopper with a fixed orifice width. The flow rate is measured averaging the downward velocity in the plug-flow region. The fitting of (a) validates the result of a dimensional analysis, $Q \propto (W-d)^{1.5}$.

Figure 6(a) shows the relation between the flow rate and orifice size in a log–log scale. When $k = 1$, the data fit to a power law scaling with an exponent of 1.48. Although $k = 0.94$ gives the exact exponent of 1.5, we do not attach much importance to the deviation as our flow rate measure is indirect. However, it is sufficient to check that the Beverloo correlation (dimensional analysis) holds in a 2D silo.

We also investigated how the funnel angle affects the flow rate. In order to compare the rate at a fixed orifice width, we interpolate the rate with $W = 18$ mm from data with $W = 16$, 20 and 24 mm for the silo experiment. Figure 6(b) shows a consistent increase in the flow rate as the angle increases. The flow rate in the 60° funnel turns out to be about 33% more than that in the flat-bottom silo. This dependence is consistent with the data from [37], although the reported increase of the flow rate is smaller than our data. We believe the increased flow rate largely comes from the fact that the smooth rigid boundary facilitates the passage of particles. As seen clearly from figures 2(b) to 5(b), the stagnant zone present in the corners of the flat-bottom silo is replaced by wedges. Thus the slip velocity at the boundary increases as the angles increase, which makes the out-going flow at the orifice ($z = 0$) more uniform and shear free. This effect appears to allow the particles to exit the orifice more easily.

4.3. Diffusion of particles in an uniform flow

As explained in section 2, particle diffusion is a key property to distinguish between different possible microscopic mechanisms for dense granular flow. The void model and the spot model predict quite similar mean flow profiles (given by the kinematic model scales much larger than the grain size), but the former predicts $b_p/b = \mathrm{O}(1)$ while the latter predicts $b_p/b = \mathrm{O}(10^{-2})$. In this section, we briefly discuss measurements of particle diffusion in our experiments, as also previously reported in [30].

To measure diffusion, the random component of particle displacement is obtained by subtracting the average component:

$$\Delta x = \Delta x' - u\Delta t \qquad \text{and} \qquad \Delta z = \Delta z' + v\Delta t, \tag{15}$$

where $\Delta x'$ (or $\Delta z'$) is the observed displacement in the x (or z) direction, Δx (or Δz) is the random displacement in the same direction, and Δt is the time gap between two consecutive

frames and can be increased by any integer multiple. The observation window is in a nearly plug-flow region far from the orifice, where u is negligible and v is almost uniform (and set by varying the orifice width).

The probability density distributions of Δx and Δz are observed to display fat tails compared to a Gaussian distribution. The statistics of Δz also show an anisotropy due to gravitational acceleration and inelastic collisions. When the width of the distributions is examined as a function of Δt, the scaling shows a crossover from super-diffusion, $\langle \Delta x^2 \rangle \propto \Delta t^{1.5}$ and $\langle \Delta z^2 \rangle \propto \Delta t^{1.6}$, to diffusion, $\langle \Delta x^2 \rangle \propto \langle \Delta z^2 \rangle \propto \Delta t$. A significant observation is that the lines of $\langle \Delta x^2 \rangle$ and $\langle \Delta z^2 \rangle$ for different v collapse into a single line when they are plotted against the distance dropped, $v\Delta t$, allowing us to characterize the dynamics only by distance moved, independent of the flow rate, v. We found that this dynamical crossover occurs after a particle falls roughly by its diameter irrespective of the flow rate.

The fact that the dynamics only depends on geometry strongly suggests that advection and diffusion have the same physical source (such as a the passage of a void or spot). It also suggests that structural rearrangements with long-lasting contacts dominate diffusion in dense granular flows, as opposed to ballistic collisions, which are central to the kinetic theory of gases. Direct evidence is that the cage-breaking length is estimated to be of the order of $100d$ from the rate of the nearest neighbour loss [30]. Our results suggest that the concept of 'granular temperature' based on thermodynamic, randomizing collisions is of dubious value in slow, dense granular flows.

Since the free volume models correctly predict the geometry dominated diffusion, we can proceed to evaluate them quantitatively. We compute the Péclet number, the dimensionless ratio of advection to diffusion, defined as

$$Pe_x = \lim_{\Delta t \to \infty} \frac{2Vd\Delta t}{\langle \Delta x^2 \rangle} = \frac{d}{b_{p,x}} \qquad \text{and} \qquad Pe_z = \lim_{\Delta t \to \infty} \frac{2Vd\Delta t}{\langle \Delta z^2 \rangle} = \frac{d}{b_{p,z}} \tag{16}$$

are interpreted as the distances (in units of d) for a particle to fall before it diffuses by a diameter in the x or z direction, respectively. The large measured values, $Pe_x = 320$ and $Pe_z = 150$, indicate that advection dominates diffusion. Since $b/d \approx 2$, we also find $w_x = b_{p,x}/b \approx 1/600$ and $b_{p,z}/b \approx 1/300$, which is consistent with the simple prediction of the spot model, $w \approx 10^{-3}$–10^{-2}. Of course, the data firmly reject the void model, which predicts $w \approx 1$, and cage breaking at the scale of one particle diameter.

5. Discussion

In section 4.1, we observed that the kinematic model with a constant parameter b is not consistent with the experiments. It was found that b depends on the height and the funnel angle. In this section, we investigate the validity of two important assumptions of the kinematic model, namely the constitutive law (1), and the generalized boundary condition (4) for the funnel geometry.

First, we directly check the constitutive law (1) using the results from our experiments. In each cell that was used for averaging the velocity, we measure the horizontal velocity u, the downward velocity gradient $\partial v/\partial x$, and therefore the diffusion length b. Figure 7 shows the distribution of the locally measured values of b. As expected, it shows a wide fluctuation scattered from $b = d$ to $3d$. When b is associated with v, we find b increases up to $3.4d$ and decreases as v increases. In other words, we observe higher b moving away from the stagnant zone and towards the fast flow regions at the centre. However, for the fastest-flow regions close to the orifice, b decreases. A reasonable implication of the increase in b is that the slightly lower density in the fast-flow region due to dilation makes horizontal movements easier. The decrease in b at higher v is perhaps related to the fact that particles undergo collisional flow

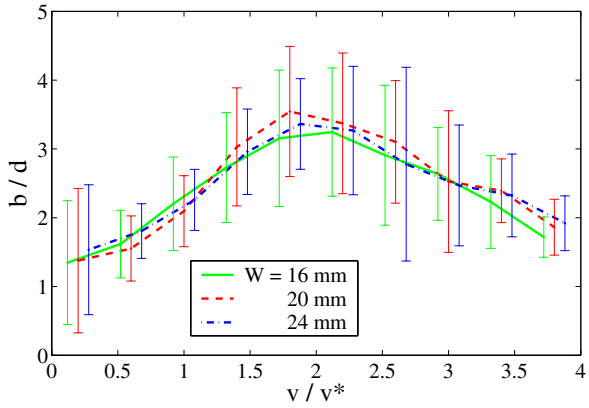

Figure 7. The locally measured diffusion length, b, as a function of the normalized velocity, v/v^*.

in the fast flowing regions near the orifice. Since the particles are less locked to neighbours than in the dense bulk away from the orifice, the shear in the downward velocity results in less horizontal movement, therefore smaller b.

A few further comments about figure 7 are in order. To collect meaningful statistics for b, we ignore shear-free zones (e.g. stagnant zone and plug-flow regions where the gradient of v is negligible), where b is likely to have large errors. We accomplish this by only considering cells where gradient is larger than 5% of the characteristic magnitude, v^*/d, where v^* is overall average velocity in the plug region. Although we only discuss b for the silo experiments in figure 7, a similar trend is also found for the hoppers as well.

The correlation between v and b gives some clues to explain the discrepancies in section 4.1. The kinematic model with constant b fails to capture the development of a more plug-like plateau in the velocity profile even with larger values of b. However, if higher b is applied to the region around the centre (where v is high), and lower b is applied to the region close to walls (where v is low), the model would come into closer agreement with experiment.

In an effort to understand the universality of this pattern, we use the overall average velocity, v^*, to normalize the downward velocity, v, from different flow rates (or orifice size). As shown in figure 7, pairs of $(v/v^*, b)$ for three different flow rates fall into nearly the same pattern. This is consistent with the trends observed in [30] that increasing the flow rate merely *fast-forwards* the entire dynamics, without changing the geometrical sequence of events.

Our way to describe our experimental results *a posteriori* is via a modified constitutive law with a variable diffusion length, b, which depends on the (scaled) local velocity:

$$u = b\frac{\partial v}{\partial x} \qquad \text{and} \qquad b = b^*\Phi\left(\frac{v}{v^*}\right), \tag{17}$$

where b^* is an effective diffusion length and Φ is a dimensionless scaling function. Note that the velocity field satisfying equation (17) is still linear with respect to rescaling the total magnitude of the velocity (by changing the total flow rate) since v/v^* is invariant when v is rescaled. However, the velocity profile in space is governed by a nonlinear diffusion equation,

$$\frac{\partial v}{\partial z} = b^*\frac{\partial}{\partial x}\left[\Phi\left(\frac{v}{v^*}\right)\frac{\partial v}{\partial x}\right]. \tag{18}$$

It is well known that spreading solutions to this equation (analogous to a concentration-dependent diffusivity) are flatter in the central region (compared to a Gaussian) when Φ is an increasing function of its argument [38].

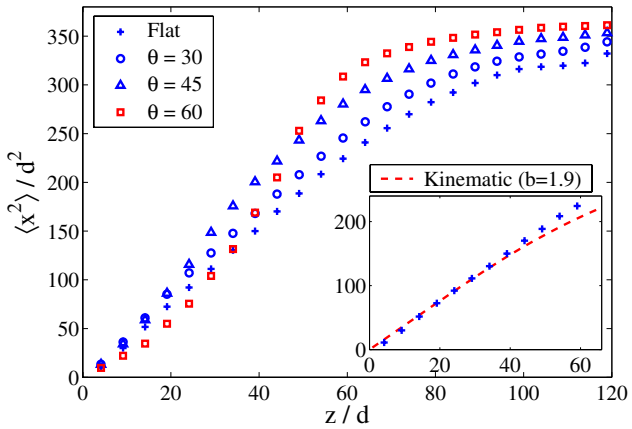

Figure 8. The variance (squared effective width) of the downward velocity profile, $\langle x^2 \rangle_v$, as a function of the vertical coordinate, z for different funnel angles.

We should consider what might be the microscopic reason for a nonlinear diffusion length in the kinematic model. In general, it would arise from interactions between different spots, which are neglected as a first approximation. It makes sense that spots of free volume should diffuse less when they find themselves in a more slowly flowing, less dense, region, with fewer other nearby spots. This could explain why b appears to grow with velocity (or spot concentration). On the other hand, the flow in the upper part of the silo becomes more plug-like and should exhibit less diffusion than the lower region of greater shear near the orifice, so it remains unclear whether the nonlinear model (17) can be given a firm microscopic justification. Further comparison with theory and experiment is needed to settle this question.

The next issue to test is the boundary condition at the side walls. Specifically, it is important to test if the model can be simply extended from open silos to hoppers by using equation (4). It is interesting to note that the curvature of the profile at $z = z_1$ around $x = 0$ remains the same for the different funnel angles (see figures 2(b)–5(b)). In fact, it is b that should increase from $b = 1.3d$ to $2.8d$ in order to reproduce the same curvature as the hopper angle is increased. For a more quantitative argument, we show in figure 8 the variance of the downward velocity profile (a measure of its squared width),

$$\langle x^2 \rangle_v = \frac{\int x^2 v(x)\,\mathrm{d}x}{\int v(x)\,\mathrm{d}x} \tag{19}$$

as a function of height, z. From equation (9), the slope of the linear regime near the orifice is equal to $2b$, and the value of the implied b does not significantly vary from $b = 1.9d$ for the silo, as can be seen in the inset to figure 8.

We conclude, therefore, that extending the kinematic model to a hopper with non-vertical walls does not seem to be successful with the naive idea of equation (4), which assumes the same bulk constitutive law holds all the way to the boundary.

It may be that a nonlinear constitutive law as in equation (17) can improve the situation because particles slip more on a funnel wall and b thus tends to be higher than in the silo. However, there may still be problems higher in the tank where the flowing region meets the vertical side walls. The boundary condition (4) requires that the strain rate (horizontal gradient of vertical velocity) vanishes at a vertical wall, and yet small velocity gradients are observed near the walls in the upper region in figures 2–5. We plan to compare the nonlinear kinematic

model, as well as other continuum models from critical-state mechanics and hourglass theory, more closely with the experimental flow profiles in future work.

6. Summary

In summary, we have used high-speed imaging techniques to track the positions of granular materials draining inside silos and hoppers. We compared our data with the continuum kinetic model and two possible microscopic theories which predict similar mean flow, the void model and spot model. These models are appealing due to their mathematical simplicity and completeness, which allows direct application to various geometries. The models also predict smooth velocity profiles, free of shock-like discontinuities, quite consistent with the experiments. Systematic deviations are observed, implying various assumptions, such as a constant diffusion length, are too simple to capture all aspects of the flow profile, but it may be that modifications can be made to improve the agreement. For example, we infer that the kinematic parameter, b, increases with the local velocity, which would imply that the spot diffusion length increases in the presence of other spots. Still, it is clear that further work is also needed to develop boundary conditions for both discrete and continuous models of slow, dense granular flows.

Acknowledgments

This work was supported by the US Department of Energy (grant No DE-FG02-02ER25530) and the Norbert Weiner Research Fund and the NEC Fund at MIT, and the National Science Foundation (grant No CTS-0334587) at Clark University.

References

[1] Duran J 2000 *Sands, Powders and Grains* (New York: Springer)
[2] Jaeger H M, Naegel S R and Behringer R P 1996 *Rev. Mod. Phys.* **68** 1259
[3] Ottino J M and Khakhar D V 2000 *Annu. Rev. Fluid Mech.* **32** 55
[4] Talbot D 2002 *MIT Technol. Rev.* **105** 54
[5] Kadak A C and Bazant M Z 2004 *Proc. 2nd Int. Topical Mtg on High Temperature Reactor Technology (Beijing, China)*
[6] Beverloo W A, Leniger H A and de Velde J V 1961 *Chem. Eng. Sci.* **15** 260
[7] Baxter G W, Behringer R P, Fagert T and Johnson G A 1989 *Phys. Rev. Lett.* **62** 2825
[8] Prakash J R and Rao K K 1991 *J. Fluid Mech.* **225** 21
[9] Nedderman R M 1992 *Statics and Kinematics of Granular Materials* (Cambridge: Cambridge University Press)
[10] Schaeffer D G 1987 *J. Differ. Eqns* **66** 19
[11] Pitman E B and Schaeffer D G 1987 *Commun. Pure Appl. Math.* **40** 421
[12] Litwiniszyn J 1958 *Rheol. Acta* **213** 146
[13] Litwiniszyn J 1963 *Bull. Acad. Polym. Sci.* **9** 61
[14] Litwiniszyn J 1963 *Bull. Acad. Polym. Sci.* **11** 593
[15] Mullins J 1972 *J. Appl. Phys.* **43** 665
[16] Mullins J 1979 *Powder Technol.* **23** 115
[17] Caram H and Hong D C 1991 *Phys. Rev. Lett.* **67** 828
[18] Nedderman R M and Tüzün U 1979 *Powder Technol.* **22** 243
[19] Tüzün U and Nedderman R M 1979 *Powder Technol.* **24** 257
[20] Mullins J 1974 *Powder Technol.* **9** 29
[21] Tüzün U, Houlsby G T, Nedderman R M and Savage S B 1982 *Chem. Eng. Sci.* **37** 1691
[22] Samadani A, Pradhan A and Kudrolli A 1999 *Phys. Rev.* E **60** 7203
[23] Medina A, Córdova J A, Luna E and Treviño C 1998 *Phys. Lett.* A **250** 111
[24] Hsiau S S and Hunt M L 1993 *J. Fluid Mech.* **251** 299
[25] Natarajan V V R, Hunt M L and Taylor E D 1995 *J. Fluid Mech.* **304** 1

[26] Menon N and Durian D J 1997 *Science* **275** 1920
[27] Savage S B 1979 *J. Fluid Mech.* **92** 53
[28] Jenkins J T and Savage S B 1983 *J. Fluid Mech.* **130** 187
[29] Hsiau S S and Hunt M L 1993 *J. Heat Transfer* **115** 541
[30] Choi J, Kudrolli A, Rosales R R and Bazant M Z 2004 *Phys. Rev. Lett.* **92** 174301
[31] Bazant M Z, Choi J, Rycroft C H, Rosales R R and Kudrolli A 2004 A theory of cooperative diffusion in dense granular flow *Preprint* cond-mat/0307379
[32] Bazant M Z 2004 The spot model for granular drainage *Mech. Mater.* at press
[33] Rycroft C H, Bazant M Z, Landry J and Grest G S 2004 The dynamics of random packings in granular flow *Preprint*
[34] Crocker J C and Grier D G 1996 *J. Colloid Interface Sci.* **179** 298
[35] MiDi G D R 2004 *Eur. Phys. J.* E **14** 341
[36] Brown R C and Richards J C 1970 *Principles of Powder Mechanics* (New York: Pergamon)
[37] Tüzün U and Nedderman R M 1982 *Powder Technol.* **31** 27
[38] Crank J 1975 *Mathematics of Diffusion* 2nd edn (Oxford: Clarendon)